

See discussions, stats, and author profiles for this publication at: <https://www.researchgate.net/publication/233851882>

Modelling of a Throttleable Ducted Rocket Propulsion System

Article in AIAA student journal. American Institute of Aeronautics and Astronautics · July 2011

DOI: 10.2514/6.2011-5610

CITATIONS

3

READS

397

4 authors, including:



Norman Hopfe

Bayern-Chemie GmbH a subsidiary of MBDA missile systems / Technische Universität Ilmenau

14 PUBLICATIONS **95** CITATIONS

SEE PROFILE

Modeling of a Throttleable Ducted Rocket Propulsion System

Christoph Bauer*, Francois Davenne*, Norman Hopfe* and Guido Kurth†

Bayern Chemie, Aschau am Inn, Germany

A throttleable ducted rocket (TDR) is a variation of a solid propellant ram jet (RC) for which the fuel mass flow rate of the solid propellant can be controlled. This is realized in such a way that the propellant has an oxygen deficient formulation which produces fuel rich combustion products within the gas generator, which will be exhausted into the ram combustor. There, these products will be further combusted with the incoming air provided by the air intakes (AI). For a TDR it is very important to model the internal aerodynamics, including the two combustion processes within the gas generator and the ram combustor, very accurately as a significant part of the operational regime can not be covered by ground tests. Therefore, the complete TDR will be here subcategorized into its main components, which can be tested individually. These sub-models will be merged into a complete system afterwards. The overall performance prediction can then be given by modeling, with a limited number of flight tests used to validate the model under real conditions.

Nomenclature

A	area
$A_{captured}$	air intake capture area
E	energy
H	enthalpy
I	impulse
M	Mach number
R	specific gas constant
SM	stability margin
T	temperature
V	Volume
a	burning rate temperature coefficient
c^*	characteristic velocity
c_p	constant pressure specific heat
c_v	constant volume specific heat
h	specific enthalpy
m	mass
n	burning rate exponent
p	pressure
r	burning rate
u	velocity
α	angle of attack
β	side slip angle
γ	ratio of specific heats
ε	dimensionless air intake mass flow ratio
ζ	inclination of the air duct with respect to the ram combustor

*R&D Engineer, Department T3R, P.O. Box 1131, D-84544 Aschau am Inn, Germany

†Technical Director of Bayern Chemie, P.O. Box 1131, D-84544 Aschau am Inn, Germany

η	air intake pressure recovery
η_λ	combustion efficiency
λ	stoichiometric air ratio
ρ	density
τ^*	residence time

Subscript

0	free stream conditions
2	end of divergent diffuser
2 <i>k</i>	inlet to ram combustor
3	beginning of combustion chamber
4	end of combustion chamber
5	critical nozzle area
<i>LSP</i>	last stable point of the air intake characteristic
<i>OP</i>	operational point on the air intake characteristic
<i>air</i>	air
<i>booster</i>	booster
<i>bp</i>	blast pipe
<i>bs</i>	burning surface
<i>com</i>	command
<i>comb</i>	combustion
<i>con</i>	control volume
<i>con2rc</i>	control volume to ram combustor
<i>dep</i>	deposit
<i>fuel</i>	fuel
<i>gas</i>	gas
<i>isv</i>	interstage valve
<i>nom</i>	nominal
<i>prop</i>	propellant
<i>prop2con</i>	propellant to control volume
<i>prop2res</i>	propellant to residuals
<i>sliver</i>	booster sliver
<i>soak</i>	soak
<i>solid</i>	solid particles
<i>t</i>	total
<i>unburnt</i>	unburnt

I. Introduction

One of the main advantages of a liquid fuel in comparison to a solid propellant ram jet is the possibility to control the thrust of the system via the fuel mass flow rate to the ram combustor. A throttleable ducted rocket (TDR) combines this advantage of active thrust control with the higher volume specific energy of the solid propellant, the high manoeuvring capability over the complete flight domain, a wide operational envelope and no risk of flame out.¹

A TDR can be divided into two combustion chambers, the so-called gas generator (GG) in which a solid propellant with oxygen deficient formulation is combusted to generate a fuel rich combustion gas. The latter is fed to the ram combustor (RC) in which the final combustion process takes place with the oxygen of the incoming air. The controllability of the gas flow from the GG to the RC is given by the fact that besides the dependency on the soak temperature of the grain T_{soak} , the burn rate r of a solid propellant is highly dependent on the static pressure at the burning surface p_{bs} . This can be described by *Vieilles* law:²

$$r = a \cdot p_{bs}^n \quad (1)$$

Based on an exact knowledge of the burnings surface A_{bs} , the steady state mass flow from the GG, respectively the control volume, to the RC \dot{m}_{con2rc} can be calculated:

$$-\dot{m}_{prop} = \rho_{prop} \cdot A_{bs} \cdot r \approx \dot{m}_{con2rc} + \dot{m}_{con} \quad (2)$$

The pressure inside the GG can be controlled via an interstage valve (ISV) which adjusts the area of the blast pipe, the connection between the GG and the RC. Under the assumption of choked conditions the mass flow through the valve can be given by:

$$\dot{m}_{con2rc} = \frac{p_{t,con} \cdot A_{isv,eff}}{\sqrt{R_{con} \cdot T_{con}}} \cdot \left(\sqrt{\gamma_{con}} \cdot \left(\frac{2}{\gamma_{con} + 1} \right)^{\frac{\gamma_{con}}{\gamma_{con} - 1}} \right) \quad (3)$$

The thrust, provided by the RC, is dependent on the already discussed fuel mass flow rate $\dot{m}_{con2rc} = \dot{m}_{fuel}$ and the air mass flow \dot{m}_{air} delivered by the air intakes (AI). The air mass flow is on the one hand dependent on the free flight conditions, like Mach number M_0 , angle of attack α and side slip β and the flight altitude which defines the static pressure p_0 and temperature T_0 . On the other hand, it is also dependent on the required total pressure inside the RC unless the supercritical branch of the AI characteristic is used. Based on the stoichiometric air ratio and the static pressure, the combustion temperature within the RC can be determined. By this the thrust of the RJ is defined as well as the already mentioned required total pressure, delivered by the AI. In addition, reasonable operation of a RJ is only possible above Mach numbers of approximately $M \approx 2.0$. Therefore, a RJ has to be accelerated from launch conditions by an additional booster.

There are two main reasons that make it mandatory to provide a detailed model of a TDR:

- Firstly, the performance of a RJ is highly dependent on the free flight conditions like Mach number, angle of attack or altitude. To cover the complete operational envelope by ground or free flight tests is not possible due to the limited number of flight tests and the fact that some of these conditions can not be simulated during ground tests. That is why it is necessary to break down the complete TDR into independent subsystems. Based on ground tests conducted with these subsystems, a mathematical sub-model can be deduced which can afterwards be integrated into a model which represents the interaction of the single subsystems. Based on this model, a performance statement for the complete envelope can be given, while the limited number of free flight tests is used solely for the validation of the model.
- Secondly, in consequence of the pressure dependent fuel mass flow to the RC, the thrust of the RJ can be controlled via the ISV. The design of such a propulsion control algorithm (PCA) requires a detailed understanding of the steady state and dynamic behavior of the PSS in order to improve the performance of the PCA by enabling a feed forward response loop and to guarantee stable conditions of the PSS.³

The current paper will discuss an approach to model the overall performance of a TDR. From the main steps to set up a simulation model⁴

- formulation of the problem
- gathering of the relevant data
- conceptual design of the model
- translation of the model concept into a source code
- verification of the correct implementation
- validation of the model

it will cover the model conceptualization by describing the several mathematical models for the main subsystems, as well as the validation by comparing different test results with the outcome of the simulation.

II. Principle Modeling of the Propulsion System

The main components of a TDR, namely the

- Booster
- Air Intakes (AI)
- Port Covers (PC)
- Gas Generator (GG)
- Interstage Valve (ISV)
- Ram Combustor (RC)

have already been addressed in the previous paragraph, except for the port covers (PC) which protect the air ducts from the hot booster gases, see figure 1.

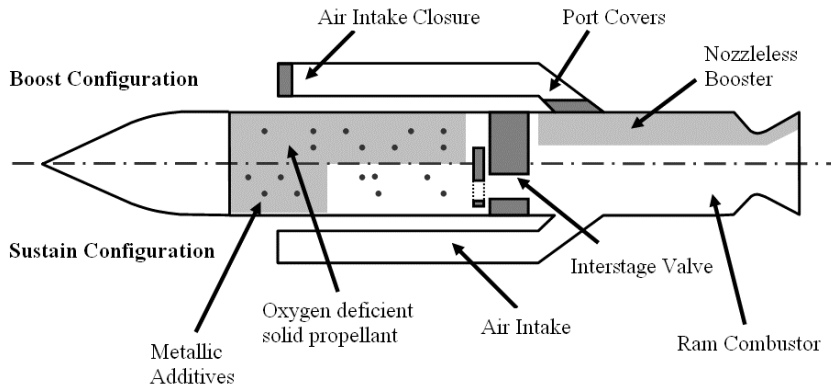


Figure 1. Main Components of a TDR for sustain and boost configuration.

To model the complete PSS these main components have to be structured in subsystems which can be modeled and tested independently. In addition, such a structure has to take into account the chronological order. In principle the operation of a RJ can be subcategorized into a boost phase in which the missile is accelerated to a reasonable Mach number, a sustain phase in which the PSS works as a real RJ and a so-called transition phase during which the configuration change takes place.

After ignition of the booster, the GG propellant is ignited automatically by hot booster gases flowing through the blast pipe. If an integrated booster, as it can be seen in figure 1 is used, the AIs have to be protected from the high temperature and high pressure booster gases by the closed PC. The AI have also to be closed to avoid buzzing during air carriage and boost phase. During the transition phase the PC and the AI are opened to led the free stream air entering the RC to deliver the oxygen which is mandatory for the final combustion during the sustain phase of the missile.

II.A. Gas Generator

As already mentioned the objective of the GG is to generate a fuel rich combustion gas mass flow which can be controlled via the valve area. The objective of the model is to simulate the dynamic of the GG namely the time dependent static pressure and the fuel mass flow rate within the GG as a function of the commanded valve position. The necessary differential equations are given by the conservation of mass and energy and by the equation of state in a predefined control volume, see figure 2. This figure shows both, the control volume (red dashed) and the incremental increase (blue dashed) due to the combustion of the propellant:

$$\dot{V}_{con} = A_{bs} \cdot r \quad (4)$$

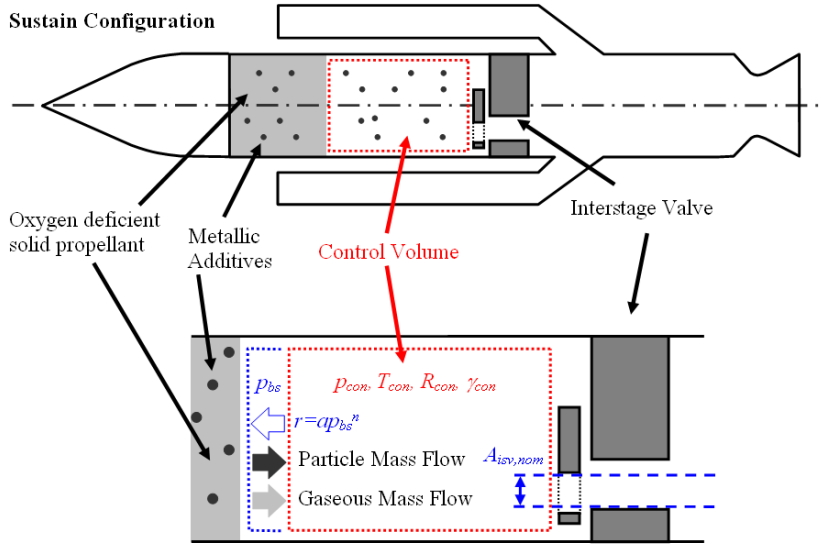


Figure 2. Control volume of the GG

To improve the performance of a TDR, the solid propellant is commonly enriched with metallic additives such as boron or aluminium which are not completely consumed during the first combustion process within the GG. Therefore, the combustion product in the GG has to be subcategorized into a particle and a gas fraction. The derivatives of the particle and the gas mass within the control volume have to be treated separately.

$$\dot{m}_{solid,con} = \dot{m}_{solid,prop2con} - \dot{m}_{solid,con2rc} \quad (5)$$

$$\dot{m}_{gas,con} = \dot{m}_{gas,prop2con} - \dot{m}_{gas,con2rc} \quad (6)$$

To calculate the derivative of the temperature in the control volume, the pressure and volume work as well as the enthalpy fluxes into and from the control volume have to be taken into account:

$$E_{con} = c_v \cdot m_{con} \cdot T_{con} \quad (7)$$

$$\dot{E}_{con} = c_v \cdot \dot{m}_{con} \cdot T_{con} + c_v \cdot m_{con} \cdot \dot{T}_{con} \quad (8)$$

$$E_{con} = H_{con} - p_{con} \cdot V_{con} \quad (9)$$

$$\dot{E}_{con} = \dot{H}_{con} - \dot{p}_{con} \cdot V_{con} - \dot{V}_{con} \cdot p_{con} = (\dot{m}_{comb,prop2con} \cdot h_{comb} - \dot{m}_{con2rc} \cdot c_{p,con} \cdot T_{con}) - \dot{p}_{con} \cdot V_{con} - \dot{V}_{con} \cdot p_{con} \quad (10)$$

$$\frac{\dot{E}_{con}}{E_{con}} = \frac{c_v \cdot \dot{m}_{con} \cdot T_{con}}{c_v \cdot m_{con} \cdot T_{con}} + \frac{c_v \cdot m_{con} \cdot \dot{T}_{con}}{c_v \cdot m_{con} \cdot T_{con}} = \frac{\dot{m}_{con}}{m_{con}} + \frac{\dot{T}_{con}}{T_{con}} \quad (11)$$

$$\dot{T}_{con} = T_{con} \cdot \left(\frac{\dot{E}_{con}}{E_{con}} - \frac{\dot{m}_{con}}{m_{con}} \right) \quad (12)$$

Finally the derivative of the static pressure can be deduced from the equation of state:

$$p_{con} = \rho_{con} \cdot R \cdot T_{con} = \frac{m_{con}}{V_{con}} \cdot R_{con} \cdot T_{con} \quad (13)$$

$$\dot{p}_{con} = \left(\frac{\dot{m}_{con}}{V_{con}} \cdot R_{con} \cdot T_{con} \right) - \left(\frac{m_{con}}{V_{con}^2} \cdot R_{con} \cdot T_{con} \cdot \dot{V}_{con} \right) + \left(\frac{m_{con}}{V_{con}} \cdot R_{con} \cdot \dot{T}_{con} \right) \quad (14)$$

$$\frac{\dot{p}_{con}}{p_{con}} = \frac{\dot{m}_{con}}{m_{con}} - \frac{\dot{V}_{con}}{V_{con}} + \frac{\dot{T}_{con}}{T_{con}} \quad (15)$$

$$\dot{p}_{con} = p_{con} \cdot \left(\frac{\dot{E}_{con}}{E_{con}} - \frac{\dot{V}_{con}}{V_{con}} \right) \quad (16)$$

$$\dot{p}_{con} = p_{con} \cdot \left(\frac{(\dot{m}_{h,prop2con} \cdot h_{comb} - \dot{m}_{con2rc} \cdot c_{p,con} \cdot T_{con}) - \dot{p}_{con} V_{con} - \dot{V}_{con} p_{con}}{E_{con}} - \frac{\dot{V}_{con}}{V_{con}} \right) \quad (17)$$

All three differential equations assume a constant specific heat ratio γ_{con} and constant specific gas constant R_{con} within the control volume.

II.A.1. Burning surface

The differential equations to calculate the time dependent behavior within the GG are given for a predefined control volume. This approach assumes that the combustion process of the GG solid propellant has already taken place and can be treated independently. As described by equations 1 and 2 the propellant mass consumption $-\dot{m}_{prop}$ is a function of the soak temperature of the grain and the static pressure at the burning surface, given by *Vieilles* law whereas the temperature coefficient a describes the dependency on the soak temperature and the pressure exponent the influence of the pressure.

$$r = function(T_{soak}, p_{bs}) = a \cdot p_{bs}^n \quad (18)$$

The *Vieilles* law is the most simple approach to describe the dependency of the empirically determined burning rate. It is also possible to improve this law by for example defining the pressure exponent as a function of the pressure:

$$n = function(p_{bs}) \quad (19)$$

These equations are based on empirical results and describe solely the burning rate of a propellant, not taking into account the amount of propellant mass which really contributes to the combustion process. In addition, it might be necessary to model additional residuals. Therefore, the overall consumed propellant mass has to be divided into several parts

$$-\dot{m}_{prop} = \rho_{prop} \cdot A_{bs} \cdot r = \dot{m}_{unburnt} + \dot{m}_{solid,prop2res} + \dot{m}_{solid,prop2con} + \dot{m}_{gas,prop2con} \quad (20)$$

The enthalpy release during the combustion process within the GG can be modeled in two different ways. The first approach is to determine the gas conditions like temperature, specific heat ratio or the specific gas constant dependent on the static pressure by equilibrium calculations. Reaction kinetics can be taken into account by modifying the reactant compositions, or more precisely by defining some of the reactants as

inert in order to avoid that these components take part in the combustion process. Based on the specific conditions during simulation, the transient conditions can be determined by interpolation.

$$(T_{comb}, \gamma_{comb}, R_{comb}) = function(reactants, p_{bs}) \quad (21)$$

$$h_{comb} = \frac{\gamma_{comb}}{\gamma_{comb} - 1} \cdot R_{comb} \cdot T_{comb} \quad (22)$$

The other approach is to define a mass specific standard heat of formation $h_{comb,0}$ via equilibrium calculations and scale this theoretical value dependent on the residence time with the GG τ^* and the pressure at the burning surface based on subsystem tests.

$$h_{comb} = function(h_{comb,0}, \tau^*, p_{bs}) \quad (23)$$

II.A.2. Valve

The previous paragraph dealt with the incoming fluxes to the control volume, while the outflow is determined by the ISV. The ISV consists of a slider which partly covers the inlet to the blast pipe, see $A_{isv,nom}$ in figure 2. Under the assumption of choked conditions, the mass flow to the RC can be calculated by:

$$\dot{m}_{con2rc} = \frac{p_{t,con} \cdot A_{isv,eff}}{\sqrt{R_{con} \cdot T_{con}}} \cdot \left(\sqrt{\gamma_{con}} \cdot \left(\frac{2}{\gamma_{con} + 1} \right)^{\frac{\gamma_{con}}{\gamma_{con} - 1}} \right) \quad (24)$$

Analogously, two options to model the flow are possible: The first option is to treat the particle laden gas of the GG as a simple generic gas which requires adjustments of either the specific gas constant R_{con} , the specific heat ratio γ_{con} or the effective valve area $A_{isv,eff}$. In alternative, the mass flux through the valve is calculated only for the gas fraction and the solid mass flux can be deduced from the given particle to gas ratio. The latter approach has to take into account the total pressure losses due to the acceleration of the particles.

The geometrical valve area $A_{isv,nom}$ is given by the position of the interstage slider. Based on the commanded ISV position ISV_{com} , specific delays and movement speed of the actuator as well as mechanical hysteresis and offsets have to be considered.

Another main topic are possible deposits within the blast pipe. Under normal conditions the nominal valve area $A_{isv,nom}$ is regarded to be the critical area. Based on empirical results, a time dependent decrease of the blast pipe area $A_{isv,bp}$ resulting from deposits can be seen, which in consequence leads to a smaller critical area than given by the slider.

$$A_{isv,dep} = \min\{A_{isv,bp}, A_{isv,nom}\} \quad (25)$$

An exact modeling of deposits is important as the effective valve area determines the static pressure inside the GG and in consequence the fuel mass flow to the RC. The maximum allowed fuel mass flow rate is limited by the stability of the AI which will be discussed in detail in the following chapter. Even if the fuel mass flow rate is no longer completely controllable if the nominal area based on the position of the slider is bigger than the remaining cross section of the blast pipe, an exact knowledge of the resulting cross section $A_{isv,dep}$ is mandatory to limit the flight conditions based on simulations to guarantee stable operation of the AIs.

II.B. Ram Combustor including the Air Intake

Based on the fuel mass flow rate determined within the GG sub model, the overall performance of the TDR can be calculated. Therefore, the gas conditions like the temperature T_4 , the specific heat ratio γ_4 and the specific gas constant R_4 after the combustion process have to be calculated to determine the total thrust of the RJ. These conditions are highly dependent on the air mass flow, thus the exact operating point on the AI characteristic is one of the main topics of the RC modeling.

The main performance parameters of a supersonic AI for a specific operational point (OP) are the dimensionless total pressure at the end of the divergent diffuser section η and the dimensionless air mass flow delivered to the RC ε . The AI performance is commonly given via an ε - η -plot, see figure 4, the so called AI characteristic dependent on the flight conditions, defined by the free stream Mach number M_0 , the angle of incidence α and the side slip angle β .

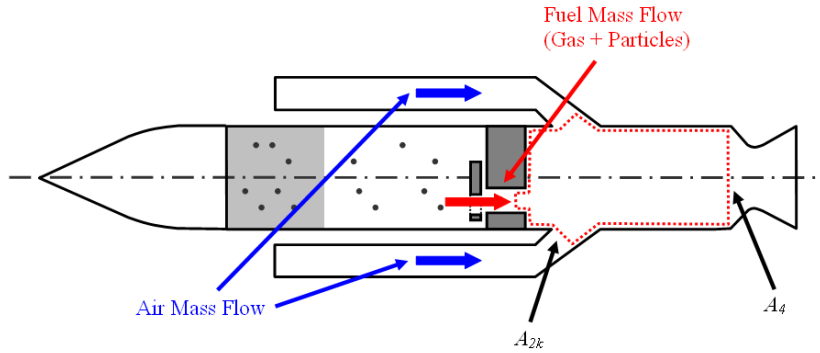


Figure 3. Control volume of the RC for conservation of impulse and mass

$$\varepsilon = \frac{\dot{m}_{air}}{\dot{m}_{theo}} = \frac{\dot{m}_2}{\dot{m}_{theo}} = \frac{\dot{m}_2}{A_{captured} \cdot u_0 \cdot \rho_0} \quad (26)$$

$$\eta = \frac{p_{t2}}{p_{t0}} \quad (27)$$

Dependent on the required total pressure the AI delivers the corresponding air mass flow defined by the characteristic. Due to the fact that the total pressure in the RC is a function of the air mass flow the determination of the AI operation point can only be done iteratively under the assumption of checked nozzle:

- Based on a predefined total pressure recovery the effective air mass flow to the RC can be determined dependent on the flight conditions.
- Based on the given air mass flow \dot{m}_{air} and the total pressure at the end of the diffuser p_{t2} the momentum at station 3 can be determined, see figure 3.

$$I_3 = p_{2k} \cdot A_3 \left(1 + \gamma_{air} \cdot M_{2k}^2 \cdot \cos(\zeta_{2k}) \cdot \frac{A_{2k}}{A_3} \right) + \dot{m}_{fuel} \cdot M_{bp} \cdot \sqrt{\gamma_{con} \cdot R_{con} \cdot T_{con}} \quad (28)$$

- Based on chemical equilibrium calculations the parameters of the combustion gas, T_4 , γ_4 and R_4 can be calculated dependent on the stoichiometric ratio λ , the combustion efficiency η_λ and the static pressure p_4 under the assumption of conservation of mass and impulse:

$$\lambda = \frac{\dot{m}_{air}}{\dot{m}_{air,stoich}} \quad (29)$$

$$\lambda_{4,eff} = \frac{\lambda_4}{\eta_\lambda} \quad (30)$$

$$(T_4, \gamma_4, R_4) = function(\lambda_{4,eff}, p_4) \quad (31)$$

$$I_4 = I_3 = p_4 \cdot A_4 + (\dot{m}_{fuel} + \dot{m}_{air}) \cdot M_4 \cdot \sqrt{T_4 \cdot \gamma_4 \cdot R_4} \quad (32)$$

- Based on the conditions at station 4 the critical area $A_{5,iterative}^*$ can be calculated:

$$A_{5,iterative}^* = \frac{c_5^* \cdot (\dot{m}_{fuel} + \dot{m}_{air})}{p_{t5}} \quad (33)$$

$$c_5^* = \sqrt{\frac{R_5 \cdot T_5}{\gamma_5 \cdot \left(\frac{2}{\gamma_5+1}\right)^{\frac{\gamma_5+1}{\gamma_5-1}}}} \quad (34)$$

- If the calculated critical area is bigger than the real nozzle throat cross section, $A_{5,iterative}^* > A_5$, the loop is repeated with the next point on the AI characteristic, which corresponds to a higher total pressure recovery and a possible lower mass flow ratio, until the critical area is equal to the nozzle throat, $A_{5,iterative}^* = A_5$.

As already mentioned the performance of the AI is described by the AI characteristic. An exact modeling of such a characteristic, either by simple algorithms or CFD is not possible. This is mainly caused by the fact that the determination of the last η - ε -combination at which a stable shock system can establish can not be done by calculations with the required accuracy.

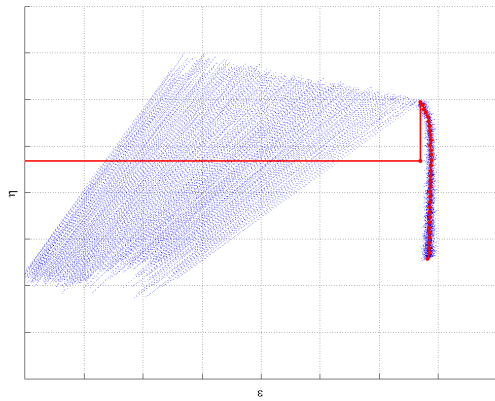
This so-called last stable point (LSP) separates the stable part of the characteristic from buzzing, defined by high frequent oscillations of the static pressure caused by a collapse of the shock system. If a configuration with more than one AI is used besides buzzing another unstable regime can establish, the so called reverse flow.⁵

Caused by either hardware tolerances or unsymmetrical flow conditions the performance of one AI always exceeds the other ones. In consequence, for some flight conditions the shock system of one AI will collapse, but will not recover. In contrary a normal shock will establish upstream of this AI caused by air streaming upstream from the RC through this AI. In contrary to buzzing which might be acceptable if the pressure amplitude is small enough reverse flow has to be avoided in all circumstances due to the fact that the air duct structure can not withstand the high temperature combustion gases.

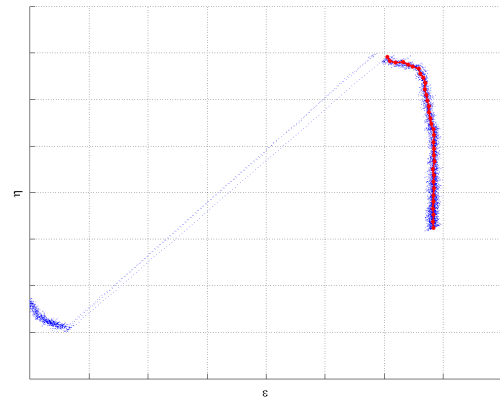
The margin between the operational point on the characteristic and the LSP is defined as the stability margin SM. Due to uncertainties in the exact flight conditions and the exact fuel mass flow rate, a minimum stability margin SM_{min} for the operation of the AI has to be defined to guarantee stable conditions.

Due to the fact that a model based prediction of the LSP is not possible the definition of the AI characteristics is done via wind-tunnel tests. The postprocessing of the data gathered during the wind-tunnel-tests results in discrete η - ε -combinations which describe the exact characteristic with the required accuracy as well as the definition whether buzz or reverse flow has to be expected, see figure 4.

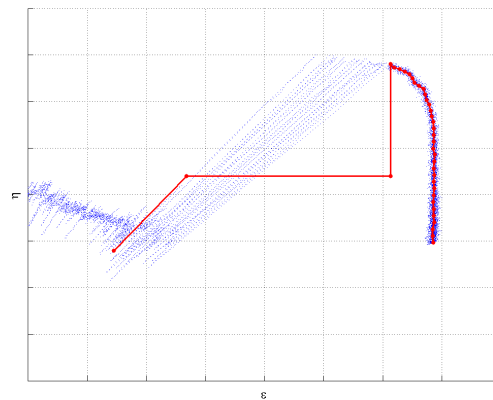
$$SM = 1 - \frac{\left(\frac{\eta_{LSP}}{\varepsilon_{LSP}}\right)}{\left(\frac{\eta_{OP}}{\varepsilon_{OP}}\right)} > SM_{min} \quad (35)$$



(a) Pure Buzz



(b) Instantaneous Reverse Flow



(c) Buzz with subsequent Reverse Flow

Figure 4. Different kinds of AI characteristics

II.C. Booster

The minimum reasonable Mach number for a RJ is in the order of $M \approx 2.0$. In consequence, the system has to be accelerated from the launch velocity to this Mach number, which is realized via a booster. This can be done either by an additional booster, for example in tandem configuration, which will be ejected after the boost phase or by a booster which is integrated to the RC structure. In the specific application the booster is an integrated nozzleless booster, which means that the critical area and the divergent section of the nozzle is defined by the booster propellant grain.

This implies that either an advanced 1D simulation of the booster propellant combustion is used to determine the performance which takes into account the geometry change due to combustion and erosion, or an empirical model is used which scales standard performance profiles based on several determining parameters.

The analysis of several booster firings has shown that the overall booster performance, given by the total impulse

$$I_{booster} = \int_{t_{booster,start}}^{t_{booster,end}} THR_{booster} dt \quad (36)$$

is constant, while the exact thrust profile is a function of the booster propellant burn rate. Therefore, based on the knowledge of the burn rate, given by *Vieilles* law

$$r_{booster} = a_{booster} \cdot p_{booster}^{n_{booster}} \quad (37)$$

and the normalized standard thrust and booster pressure profile given by different tests the exact booster thrust can be given.

The boost and the sustain phase are separated by the transition phase in which the configuration of the missile changes. This means the AI and the PC are opened to led the air stream into the RC. This transition sequence needs an exact knowledge of the remaining booster slivers. The performance of the AI is limited by the LSP. In consequence, the opening timing for the AI and the PC has to be chosen in such a way that the conditions within the RC do not lead to either buzzing or reverse flow due to high booster mass flow caused by the opening of the PC and the AI. The opening leads on the one hand to an increase of the static pressure within the RC which causes a higher booster mass flow due to the pressure dependent burn rate. On the other hand the incoming air also increases the booster mass flow by an increased erosion rate. Due to the wide flight envelope this can not be covered by a empirical model, therefore the booster slivers are covered by the RC model.

In case of booster slivers the conditions within the RC are in addition dependent on the booster sliver mass flow $\dot{m}_{booster,sliver}$.

$$\dot{m}_{booster,sliver} = A_{booster,sliver} \cdot \rho_{booster,sliver} \cdot a_{booster} \cdot p_4^{n_{booster}} \quad (38)$$

$$(T_4, \gamma_4, R_4) = function(\lambda_{4,eff}, p_4, \dot{m}_{fuel}, \dot{m}_{booster,sliver}) \quad (39)$$

III. Validation

III.A. Test Configurations

The complete PSS is subcategorized into several sub-systems which can be modeled and tested separately. These sub-system tests are necessary, both for the set up and for the validation of the model. In total five kinds of test configuration are possible:

- GGCV (Gas Generator Controlled Valve) tests consist only of the GG including the ISV. An additional chamber with a fixed throat downstream of the GG gives the opportunity to monitor the final fuel mass flow out of the GG. These test provide a very efficient way to investigate the dynamic behavior within the GG.
- CPT (Connected Pipe Transition) tests represent the complete PSS except the AIs. For a free flight trials the air mass flow, delivered by the AIs is dependent on the conditions within the RC whereas for a CPT test a predefined air mass flow with given total temperature is delivered to the RC via connected pipes. One of the main advantages of this test configuration is that the delivered air mass flow is independent from the combustion process which results in an exact knowledge of the specific stichometric air mass flow ratio λ_4 . This enables, based on the measurement of the thrust, to determine the combustion efficiency. The latter, as already mentioned, is dependent on the stoichiometric ratio λ_4 and the static pressure inside the RC, which can also be recorded during tests.

- CPE (Connected Pipe Ejector) test are comparable to CPT tests, but overcome the problem that for CPT test the static pressure at the nozzle exit is identical to the ambient pressure at the test facility. Due to the fact that the simulated flight altitude is mainly affected by the conditions of the incoming air several altitudes can be represented by the CPT tests if the nozzle throat is choked. But for specific tests it is mandatory to reduce the static pressure at the nozzle exit via an additional ejector to allow a very low static pressure within the RC, which corresponds to very low fuel mass flow in high altitudes.
- QFJ (Quasi Free Jet) tests give the opportunity to test the complete system, including the AI for specific Mach numbers. An air jet is produced which delivers a specific Mach profile under test facility altitude conditions to the AIs. These tests are of great interest for the validation of the transition sequence. In addition, possible performance differences between CPT and QFJ tests can be investigated. The latter are more representative with respect to free flights. But due to the limitation to sea level tests and to a limited number of possible Mach numbers at the QFJ-test facility, the CPT test are necessary to cover the complete flight envelope.
- Free flight test show the behavior of the PSS under real conditions, for example realistic vibrations and accelerations. Because of the limited number, the objective of the free flight tests is mainly to validate the complete PSS model, deduced from the sub system tests.

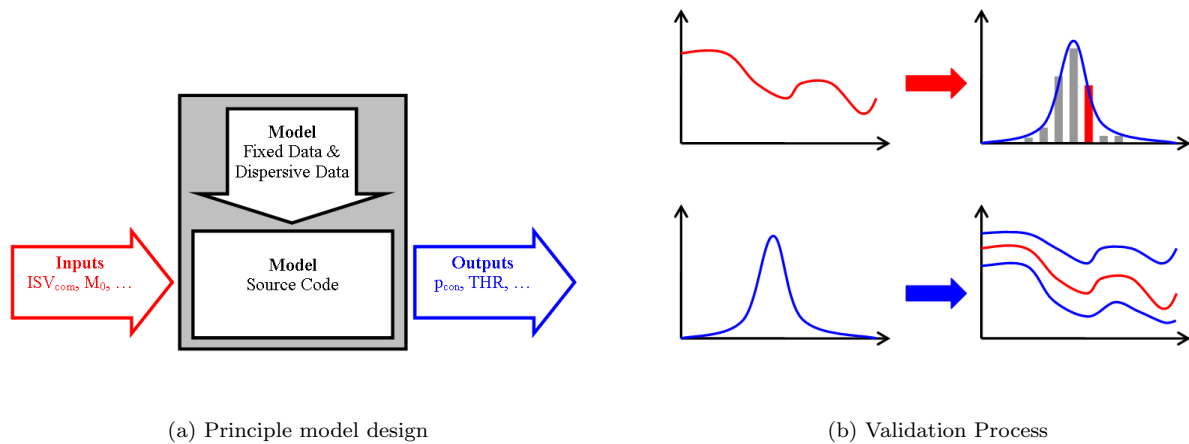


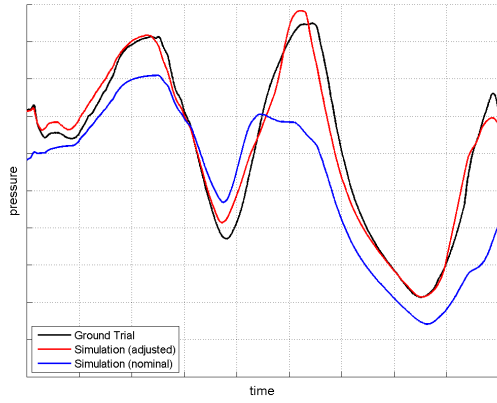
Figure 5. Model Concept

Figure 5(a) shows the principle concept of the model. Each model or sub model consist of a mathematical description, given by the source code, and the corresponding data set, either fixed or dispersed. Based on given inputs, e.g. the commanded position of the valve ISV_{com} , the corresponding outputs, in this case the effective cross section $A_{isu,nom}$ can be calculated, using the model specific parameters.

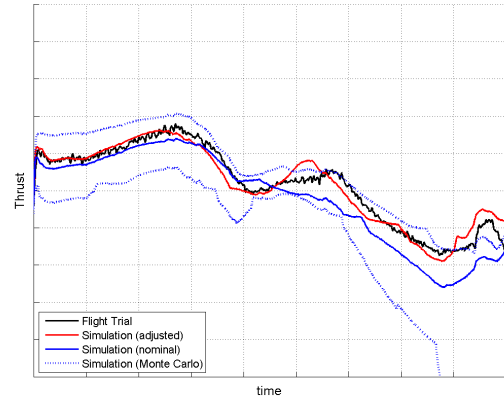
The objective of the validation is both to approve the mathematical discription and to confirm that the dispersive parameters are within the boundaries and the probability given by the distribution. The principle concept is shown in figure 5(b). For each of the dispersed parameters a distribution, either rectangular or Gaussian can be defined which will be used during Monte Carlo runs. One option for the validation is to adjust the parameters in such a way that the measured values (red) can be remodeled. Afterwards it has to be confirmed that the dispersive parameter (red) is within the expected distribution (blue), see figure 5(b) top. Another possibility is to show that the outcome of a test (red) is within the corridor defined by Monte Carlo runs (blue), using the corresponding distribution (blue), see figure 5(b) bottom.

III.B. Ground Trial (CPT)

The main advantage of a CPT test is that the incoming air and therefore the corresponding stoichiometric air ratio λ is independent from the conditions within the RC. In consequence the combustion efficiency and so the achieved thrust can be determined very exactly. Figure 6(a) shows the measured static pressure within the GG (black), respectively the control volume, the outcome of the simulation with nominal settings (blue) and the simulated pressure after adjusting some of the dispersive parameters (red). The static pressure is



(a) Static pressure p_{con}



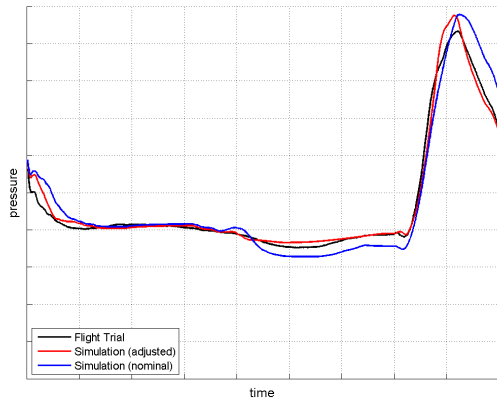
(b) Thrust THR

Figure 6. Ground trial

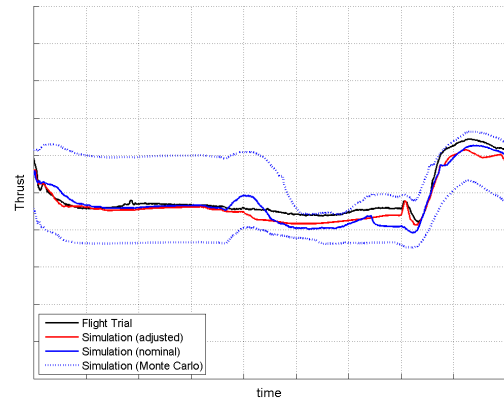
mainly dependent on the effective cross section between the GG and the RC, the consumed propellant mass, given by the burn rate r and the burning surface A_{bs} , and the amount of propellant which stays unburnt $\dot{m}_{unburnt}$.

Figure 6(b) presents the same curves for the thrust. In addition, the corridor defined by Monte Carlo runs is given in this graph (blue-dotted). Because the air mass flow is defined by the test facility the thrust is only dependent on the fuel mass flow rate \dot{m}_{fuel} . It can be seen that in this specific test the measured pressure under nominal conditions is slightly above the simulated one. This is caused by a marginal inclination of the burning surface of the end-burner which causes a slightly increased burning surface. This is also approved by the close match in the thrust and the correct simulation of the burn-out, which is not covered by the plots.

III.C. Free Flight Trial



(a) Static pressure p_{con}



(b) Thrust THR

Figure 7. Flight trial

Besides the fact that the air mass flow is known exactly during a CPT test in comparison to a free flight test, the measured thrust is more accurate. The final thrust during a free flight test is deduced from the acceleration, considering the corresponding drag and the overall mass of the missile. But only during a free

flight test the behavior of the RJ can be investigated under real conditions, e.g. vibrations, accelerations.

In addition a validation of the AI performance modeling can only be done by free flight test. On the QFJ test facility only limited number of Mach numbers at $\alpha = 0$ and $\beta = 0$ can be tested. In addition the QFJ tests are restricted to sea level conditions. Another point is that at the QFJ test facility it is not possible to reach unstable conditions of the AI, either buzzing or reverse flow. Therefore, during one free flight trial, the flight conditions like angle of attack α or side slip angle β were set in such a way that based on simulations reverse flow should have happened. The subsequent post processing of the trial gave evidence that reverse flow happened by several pints.

- At the specific point in time the simulated SM got zero
- The measured thrust shows a sudden decay which is caused by the reduced air mass flow and the increased drag
- The sudden change of the aerodynamic forces was compensated by the fins to hold the commanded side slip angle

Analogue to the ground trials figure 7 shows the results gathered during a free flight test (black) and on the other hand the simulation results, after an adjustment of the parameters (red), for nominal settings (blue) and the upper and lower limit of 50 Monte Carlo runs (blue - dashed).

IV. Conclusions

An exact modeling of the performance of a TDR propulsion system is mandatory because of two reasons. First of all the performance, namely the thrust, is highly dependent on the flight conditions of the missile such as altitude, Mach number or angle of attack. Therefore, it is not possible to cover the complete flight domain either by ground or free flight. In consequence, a performance prediction can only be given via a simulation tool. The second reason is the possibility of an active thrust control, since a detailed understanding of the processes within the TDR are mandatory for the design of the control algorithm.

To set up a model for a TDR the complete system has to be subcategorized into its main components the booster, the GG, the ISV, the RC, the AIs and the PCs. The current paper describes several model concepts, including the continuous modeling of the combustion process within the GG, the final mass flux to the RC, the empirical model of a booster and the determination of the overall thrust based on the equilibrium calculations within the RC.

The principle concept is to test these components independently, in order to set up a model concept based on the gathered data, to translate this concept into computer code and to merge the single sub systems into a complete model. After the correct implementation is verified the model can be validated on the bases of further test. The objective of the validation is the confirmation of both the correct modeling concept and the model specific parameters. During the validation process it has to be shown that the dispersive parameters of the model are within the defined probability distribution. In addition it can be checked whether the results of further tests are within a corridor given by Monte Carlo runs based on these distributions. Such a validation process is shown in this paper via a free flight trial and a CPT test.

The post processing of the presented trials shows that it is possible to model the combustion processes with a TDR very accurately. A very close match of the thrust and the pressure profile can be achieved by small adjustments of the specific parameters. In consequence, based on this model, a thrust prediction can be given for the complete flight domain. To take into account the model dispersions Monte Carlo runs can be conducted, in order to provide an impression of the tolerances on thrust and pressure that has to be expected.

The exact understanding of all the processes of a TDR gives on the one hand the possibility for an optimization, in which different configurations can be simulated and sensitivity studies conducted. On the other hand, a detailed model can support the analysis of possible problems or malfunctions.

References

- ¹Besser, H. L., Weinreich, H. L., and Kurth, G., "Fit for Mission - Design Tailoring Aspects of Throttleable Ducted Rocket Propulsion Systems," *44th AIAA/SME/SAE/ASEE Joint Propulsion Conference and Exhibit*, AIAA, Hartford, CT, July 2008.
- ²Besser, H. L., "History of Ducted Rocket Development at Bayern-Chemie," *44th AIAA/SME/SAE/ASEE Joint Propulsion Conference and Exhibit*, AIAA, Hartford, CT, July 2008.
- ³Pinto, P. C. and Kurth, G., "Robust Propulsion Control in all Flight Stages of a Throttleable Ducted Rocket," *47th AIAA/SME/SAE/ASEE Joint Propulsion Conference and Exhibit*, AIAA, San Diego, CA, August 2011.
- ⁴Banks, J., *Handbook of Simulation*, John Wiley and Sons, Inc., New York, 1998.
- ⁵Bauer, C. and Kurth, G., "Air Intake Development for Supersonic Missiles," *44th AIAA/SME/SAE/ASEE Joint Propulsion Conference and Exhibit*, AIAA, Hartford, CT, July 2008.